Design and Performance Evaluation of a Portable Chamber for Prevention of Aerosol Airborne – Infection

Fatma AbdelMordy Kassem[1,*], Ahmed Farouk AbdelGawad[2], Ali Elsayed Abuel-Ezz[3], Mofreh Melad Nassief[2], Mohamed Adel[2]

1   Department of Volume and Fluid Flow Metrology, National Institute of Standards (NIS), Giza, Egypt
2   Department of Mechanical Power Engineering, Faculty of Engineering, Zagazig University, Egypt
3   Department of Force and Material Metrology, National Institute of Standards (NIS), Giza, Egypt

ARTICLE INFO	ABSTRACT
	Since the emergence of the COVID-19 pandemic, complications for healthcare workers in hospitals have increased. Healthcare workers have had to develop innovative solutions to deal with the shortage of resources and isolation rooms for those infected with the coronavirus. One of the solutions used is to convert the general patient room into a negative pressure room to prevent airborne infections from leaking into the surrounding environment. However, this was not always easy due to many limitations, such as the overall design of the chamber and the unavailability of mechanical parts to create negative pressure. Another solution is to use medical masks. However, they are not appropriate, especially for patients who suffer from breath shortness. With all these problems, a simple solution was reached in the present work, which is to create a portable isolation room that is simple in terms of cost and implementation. The objective was to investigate the dispersion of the infection inside the portable chamber in addition to its effectiveness in minimizing the risk of infection for healthcare workers. Thus, the airborne infection is eliminated by connecting the exit of the portable chamber directly to a vacuum pump. In the present study, a comparison was made between a normal room without a portable chamber and another with a portable chamber. Six different strategies were applied to remove pollutants. The results showed that strategy 6 was more effective than other strategies (2, 3, 4, and 5) by percentages of 61.6%, 70.4%, 52.4%, and 33.0%, respectively.

1. Introduction

The COVID-19 outbreak spread rapidly across the world at the end of 2019. The transmission of the COVID-19 virus was evaluated through practical experiments. It was concluded that the disease is spread by droplets during the exhalation of a sick person through coughing, sneezing, talking, and direct contact with an infected person [1-2]. The scattering of droplets is very important in the spread of this virus, and there are often droplets with a diameter of 0.7 microns [3]. The risk of transmission

of an airborne infection by inhalation or ingestion to people surrounding the patient has been confirmed by the World Health Organization. Therefore, it was recommended to wear medical masks and maintain a social distance of about 1 m [4]. Moreover, the outbreak has increased the risk of transmission from patients to healthcare workers. Therefore, the patient must be isolated in rooms with negative pressure to contain infectious diseases and inhibit the transmission process [5]. There are many studies on ways to prevent COVID-19 infection by natural or mechanical ventilation, including heating and air conditioning (HVAC) systems and optimal and poor use of ventilation systems [6-8]. The patient's body is to be isolated completely or partially using a plastic cover and using negative pressure generation devices in the area to isolate the patient's exhalation from spreading inside the room to control transmission [9]. Many researchers have explained the active elimination of fine particles from the air [10-12]. From research, it was found that there is evidence that COVID-19, when suspended in air, is sensibly easy to inactivate using ultraviolet (UV) light, solar radiation, UV+ filters, fibrous filters, and hybrid electrostatic filtration systems (HEFS) [13-15]. Others investigated indoor pollutants and interior smart ventilation systems [16]. The transmission of infection depends on the airflow generated by the ventilation system and internal turbulence. Disturbances in the internal environment are usually uncontrollable and can affect the room's ventilation system. Internal disturbances can arise from human activity (walking, moving, sudden opening and closing of a door, and the type of door; hinged or sliding) [17-19]. The evaporation influence can be neglected for particles in the size range of 0.5 to 20 μm [20,21]. Particles of large diameter fell to the floor because of gravity, while small ones are suspended in the indoor air at high positions [22]. Fine droplets of small size lower than 20 μm are distributed within indoor air, while coarse ones larger than 45 μm drop on the surfaces [23]. Inlet and outlet air locations significantly affect the diffusion of infectious particles in the indoor environment and office [24-25]. Additionally, one of the solutions used to protect children from the coronavirus is the use of activated carbon filters [26]. Finally, during the isolation room design for respiratory diseases, environmental conditions should be considered, such as the velocity around the patient not exceeding 0.25 m/s and carbon dioxide less than 1000 ppm [27].

In response, the present research investigates the performance of various pressure differences inside a portable chamber for the prevention of aerosol airborne infection. The primary goals of the investigation are to get rid of the epidemic, protect the medical staff in hospitals, and remove unwanted emissions in offices using negative pressure [28]. Thus, the present work tests and evaluates several strategies experimentally and computationally under different conditions.

2. Experimental Work
2.1 Room Design and Flow Measurement

Experiments were carried out in a full-scale chamber with dimensions $2.0 \times 2.0 \times 2.0$ m^3, with one air exhaust and one air inlet, as shown in Figure 1. For the room, the dimensions of the inlet and outlet openings were 0.60×0.20 m^2 and 0.35×0.35 m^2, respectively. The air supply was mounted in the wall near the ceiling and the outlet was mounted in the side wall to the left of the patient above the floor by 0.25 m according to many famous international hospitals. The isolation room was illuminated by a light of 18 W/m^2. The study had a patient length of 1.7 m lying on a bed at a height of 0.7 m from the floor, 0.8 m (W), and 1.8 m (L). During the experiments, the ventilation system supplied air at 22°C ± 0.035°C and the air change per hour (ACH) was 27 according to Eq. (1).

To achieve stable (steady state) conditions, the room was allowed to equilibrate for an hour before taking measurements. In the experiments, the manikin (patient) exhaled through the nose. The nose area was 7.85×10^{-5} m^3. The respiratory volume was 9 l/min, and the breathing frequency

was 15 per minute. The concentration of the tracer gas (CO_2) was measured continuously from 400 ppm to 29,206 ppm using air–quality sensors at four locations. Two sampling points (P1 and P2) were installed inside the room around the patient bed at 1.0 m from the floor level to evaluate the concentration of CO_2. One sampling point (P3) was located near the bed at 1.4 m from the floor level, at the same level as the healthcare worker. The final sampling point (P4) was installed at the exhaust grille to evaluate the amount of CO_2 removed from the room, as shown in Figure 1(a).

$$\text{ACH} = \frac{\text{volume flow rate at inlet } (^{m^3}/_{hr})}{\text{room volume (m}^3)} \qquad (1)$$

2.2 Portable Chamber Design

Experiments were carried out in a full-scale chamber with dimensions $0.60 \times 0.65 \times 0.55$ m^3, with an air exhaust location behind the patient with a diameter of 0.07 m, as shown in Figure 1(b). The walls of the chamber were well insulated during the experimental measurements using a plastic sheet.

To test the performance of the portable chamber, carbon dioxide was used as a "tracer gas" at 21 °C, and its volume rate was 0.6 liters per exhalation (exhalation rate was 15 times per minute). The flow rate was controlled using a rotameter mounted on the carbon dioxide gas cylinder in the testing room next to the patient's bed. Carbon dioxide concentration was ranging up to 3,000 ppm. Portable room efficiency was tested by the generation of negative pressure at a value of -1 Pa using a 3 hp-vacuum pump that was installed outside the room to avoid noise, as shown in Figure 1(c). Table 1 explains the different strategies that were applied in the present study for the prevention of aerosol airborne infection.
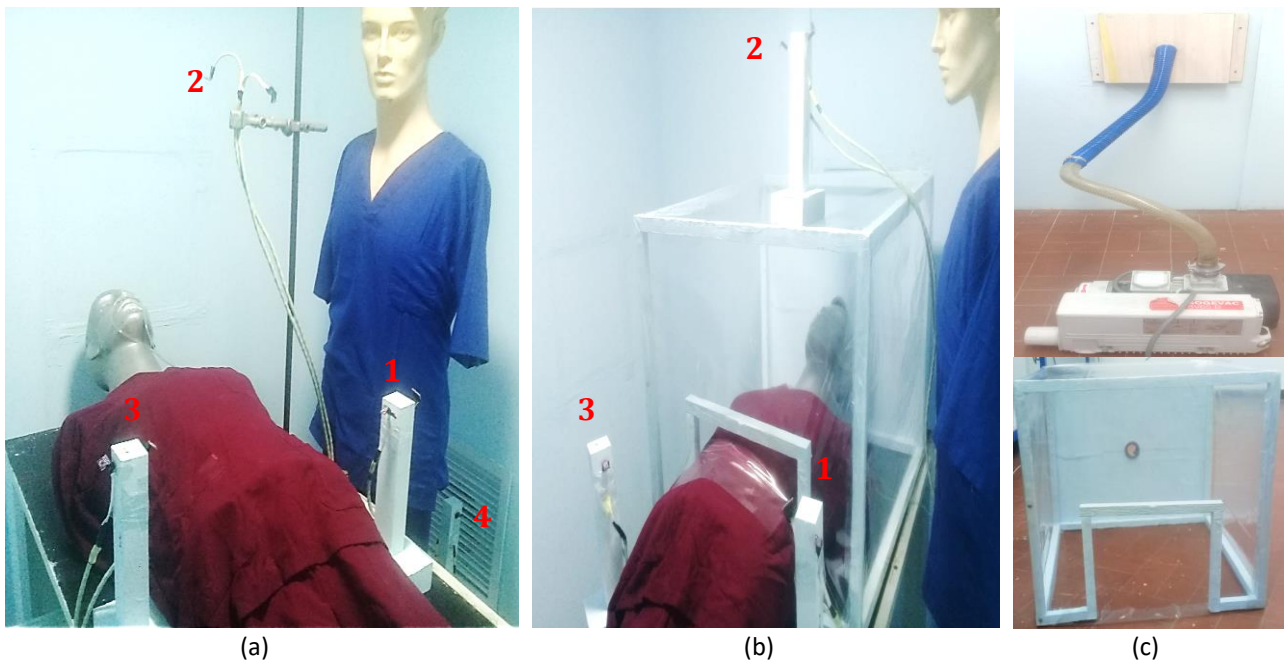
Fig. 1. (a) Measuring points (b) Portable chamber (c) Vacuum pump

Table 1
Different strategies of the present study, ACH= 27

Strategies	Description
Strategy 1	A room without a portable chamber (P_1=0 Pa)
Strategy 2	Room with a portable chamber above the patient (P_1= 0 Pa, P_2= 0 Pa)
Strategy 3	Room with a portable chamber above the patient with negative outlet pressure P_2 (P_1= 0 Pa, P_2= -1 Pa)
Strategy 4	Room with a portable chamber above the patient with negative outlet pressure P_2 (P_1= 0 Pa, P_2= -2.5 Pa)
Strategy 5	Room with a port able chamber above the patient with negative outlet pressure P_2 (P_1= 0 Pa, P_2= -5 Pa)
Strategy 6	Room with a portable chamber above the patient with negative outlet pressure P_2 (P_1= 0 Pa, P_2= -8 Pa)

3. Computational Simulation

3.1 Design Model and Grid Independence Test

The computational model was designed as a full-scale one, as shown in Figure 2. The mesh was constructed from unstructured cells to maintain a preferable mesh quality (Figure 3(a)). The results of the mesh-independence test for four mesh sizes are presented in Figure 3(b), where V is the velocity magnitude of room air that was monitored at a specific location (significant line) close to the healthcare worker along the Y-direction. The velocity values at the monitored points for the case of 1,601,892 cells with a maximum size element is 45 mm were quite close to those for the case of 1,944,132 cells with a maximum size element of 35mm because the change in element size between these cases barely affects the solution. Moreover, the relative differences in the average velocity between Cases 1 and 2, Cases 2 and 3, and Cases 3 and 4 were found to be 2.79%, 1.68%, and 0.38%, respectively. It is evident that increasing the number of cells increases the solution accuracy. It can also be concluded that the mesh system reached an independent solution in Case 4. Therefore, the mesh size of 1,944,132 cells was found to be adequate and was utilized in the present study. The details of the mesh properties are shown in Table 2.

Table 2
Mesh properties

Specification	Value
Element minimum size (mm)	0.25
Element maximum size (mm)	35
Growth rate	1.2
Curvature normal angle (deg.)	18
Inflation transition ratio	0.272
Inflation number of layers	5
Number of elements	1,944,132
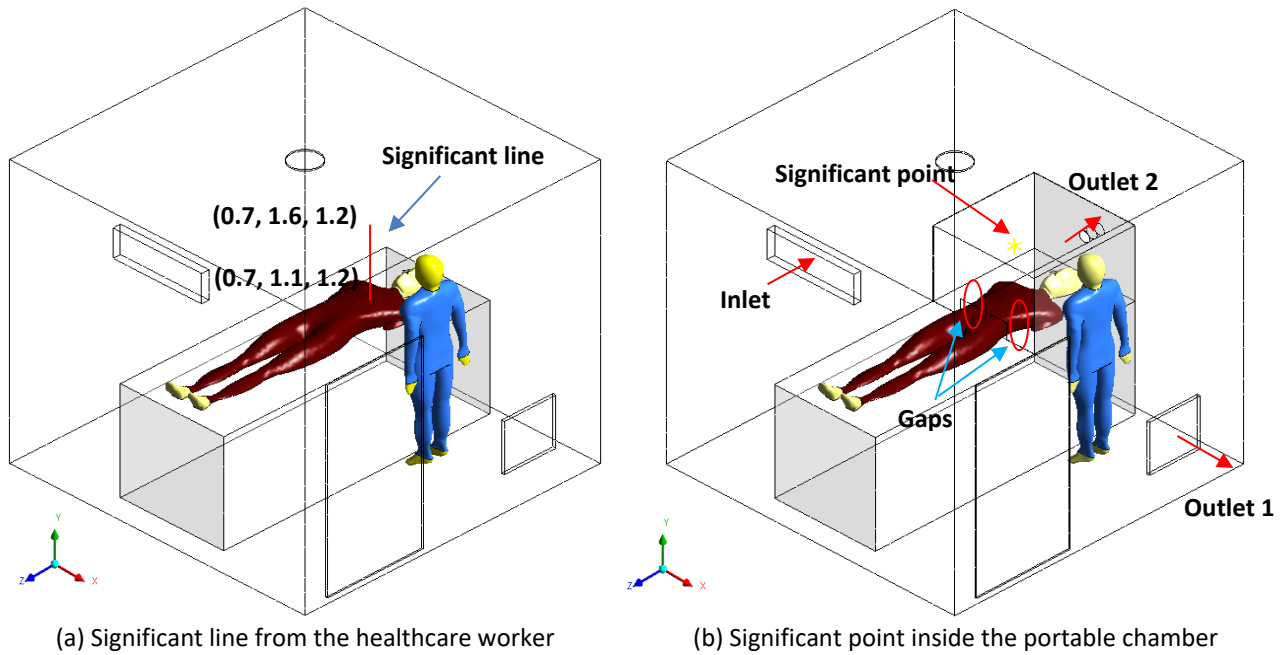
(a) Significant line from the healthcare worker   (b) Significant point inside the portable chamber
Fig. 2. Geometry of the room and computational domain
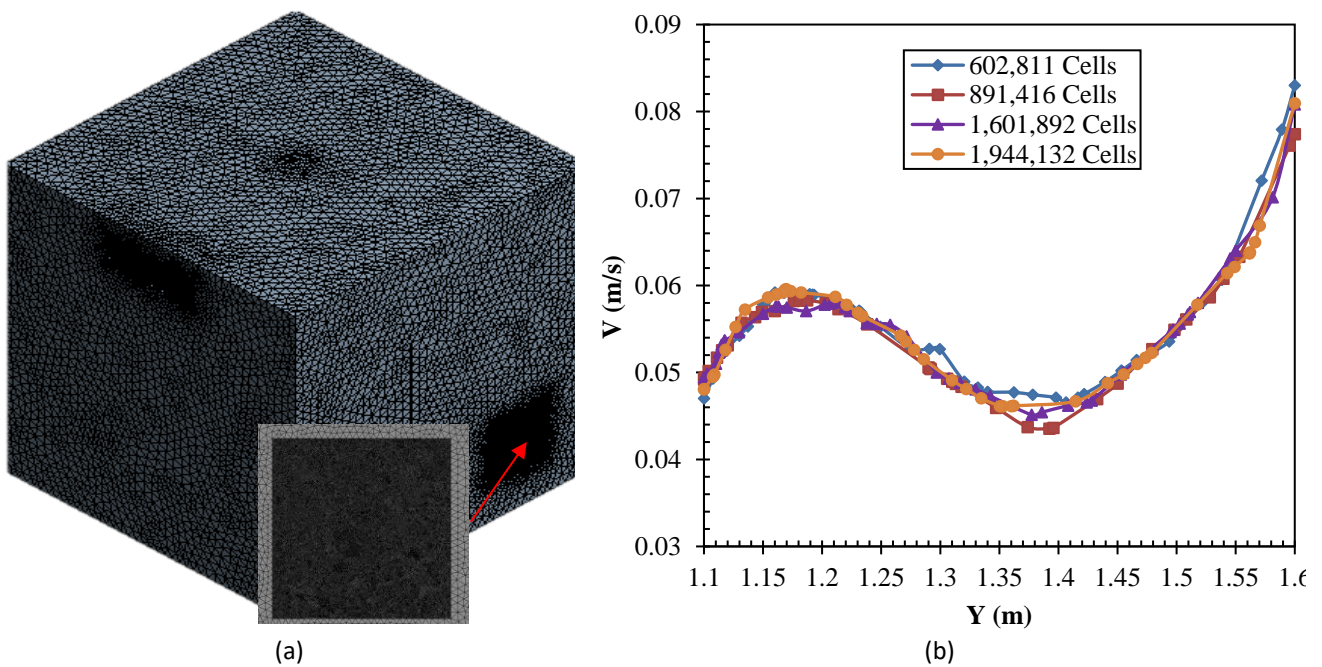
(a)   (b)
Fig. 3. (a) Mesh configuration. (b) Mesh-sensitivity analysis at the significant line from the healthcare worker

3.2 Boundary Conditions

As the dynamics of the inhalation flow close to the nose are periodic, a sinusoidal velocity is applied to the boundary condition for the mouth of the patient, as shown in Table 3. The computational simulation was carried out in the ANSYS Fluent 2016 software package. Using this package, the governing equations in three-dimensional form; the continuity equation, and momentum equations with the k-ε RNG turbulence model were solved [29] with transient analysis. The influence of relative humidity and temperature can be neglected on the diffusion of the particles with sizes ranging from 0.1 to 200 μm that emerge from the infected patient during sneezing, coughing, and talking [30–32]. In this study, the size range of the breathing particles is 0.5 – 2.5 μm,

with an average diameter of 1 µm [33]. Additionally, the velocity boundary condition at the patient's mouth is a semi-sinusoidal function according to [34-35].

The transient computations converged at residuals of 10^{-4} for the governing equations of mass, momentum, k (turbulent kinetic energy), and ε (turbulence dissipation rate), while the energy equation converged at a residual of 10^{-6}. Each transient simulation was carried out for 60.3 s with a time-step of 0.05 s and 27 ACH.

Table 3
Boundary conditions for CFD simulation

Condition	Type	Value
Supply air	Velocity inlet	Velocity: 0.5 m/s
	Discrete phase: escape	Temperature: 295 ºK
		Concentration: 0
Room exhaust air	Pressure outlet	Pressure: 0 Pa
	Discrete phase: escape	Temperature: 298 ºK
Portable chamber exhaust air	Pressure outlet	Pressure: 0, -1, -2.5, -5, -8 Pa
	Discrete phase: escape	Temperature: 298 ºK
Exhaled air by patient	Velocity inlet	V=1.99×sin((3.14/2)×t)
	Discrete phase: escape	Temperature: 300 ºK
		Concentration: 3000 ppm
Patient, healthcare worker, and bed	Wall	Adiabatic
Bio-aerosol	DPM: Injection	Velocity: 0 m/s
		Flow rate: $1 \times 10^{-5} kg/s$
		Particle Size: 0.5–2.5 µm, median 1 µm
		Density: 998.2 kg/m³

4. Results and Discussion

4.1 Validation Comparison of the Experimental and Numerical Models

The mean CO_2 concentrations for the experimental results and CFD simulation results are shown in Figure 4. There is a good agreement between the experimental and computational results. The percentage of the mean variance between the simulation and measured results is 12%. The mean uncertainty from the measured results is ± 2.0 ppm according to the uncertainty analysis, as shown in Table 4.

Table 4
Uncertainty estimation from the air quality sensor

Components	Dimension	Distribution	Divisor	Standard Uncertainty
Repeatability u_{Rep}	ppm	Normal	1	0.577
Master meter u_M	ppm	Normal	1	0.50
Resolution u_{Res}	ppm	Rectangular	$\sqrt{3}$	0.288
Drift u_D	ppm	Normal	1	0.20
Combined uncertainty $u_c = \sqrt{u_{Rep}^2 + u_M^2 + u_{Res}^2 + u_D^2}$				0.8402
Expanded uncertainty $U = K \times u_c$				1.68
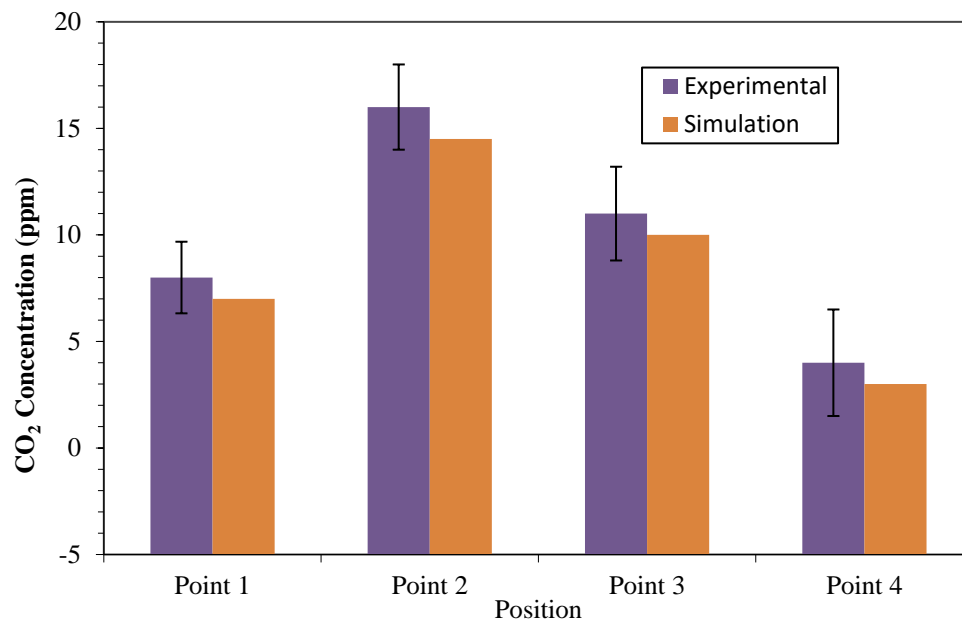
Fig. 4. Comparison between experimental and simulation results after 30 sec for strategy 1

4.2 CO_2 Concentration

According to the occupational safety and health administration (OSHA), the maximum contaminant of CO_2 in indoor air is equal to 1000 ppm [27, 36]. In this study, carbon dioxide concentration was measured inside the room using four sampling points (P1, P2, P3, and P4) by a computerized system. The average reference value of CO_2 inside the room, taken before operating the experiment and before CO_2 injection as the airborne gas, was 410 ppm. The tracer gas (CO_2) was used to monitor how concentrations were removed. Figure 5 shows the air in the indoor environment for strategies 1, 2, and 3. Due to some practical constraints, the experimental work was only possible for strategies 1, 2, and 3. However, the other strategies (4, 5, and 6) were simulated computationally. The pressure inside the room was 0.3 Pa with 27 ACH. For strategy 3, patient exhalation did not mix or diffuse inside the room, but was quickly sucked through the exhaust of the portable chamber placed behind the patient's head. This is because the patient's exhalation was controlled by the portable chamber due to the pressure difference created by the vacuum pump.
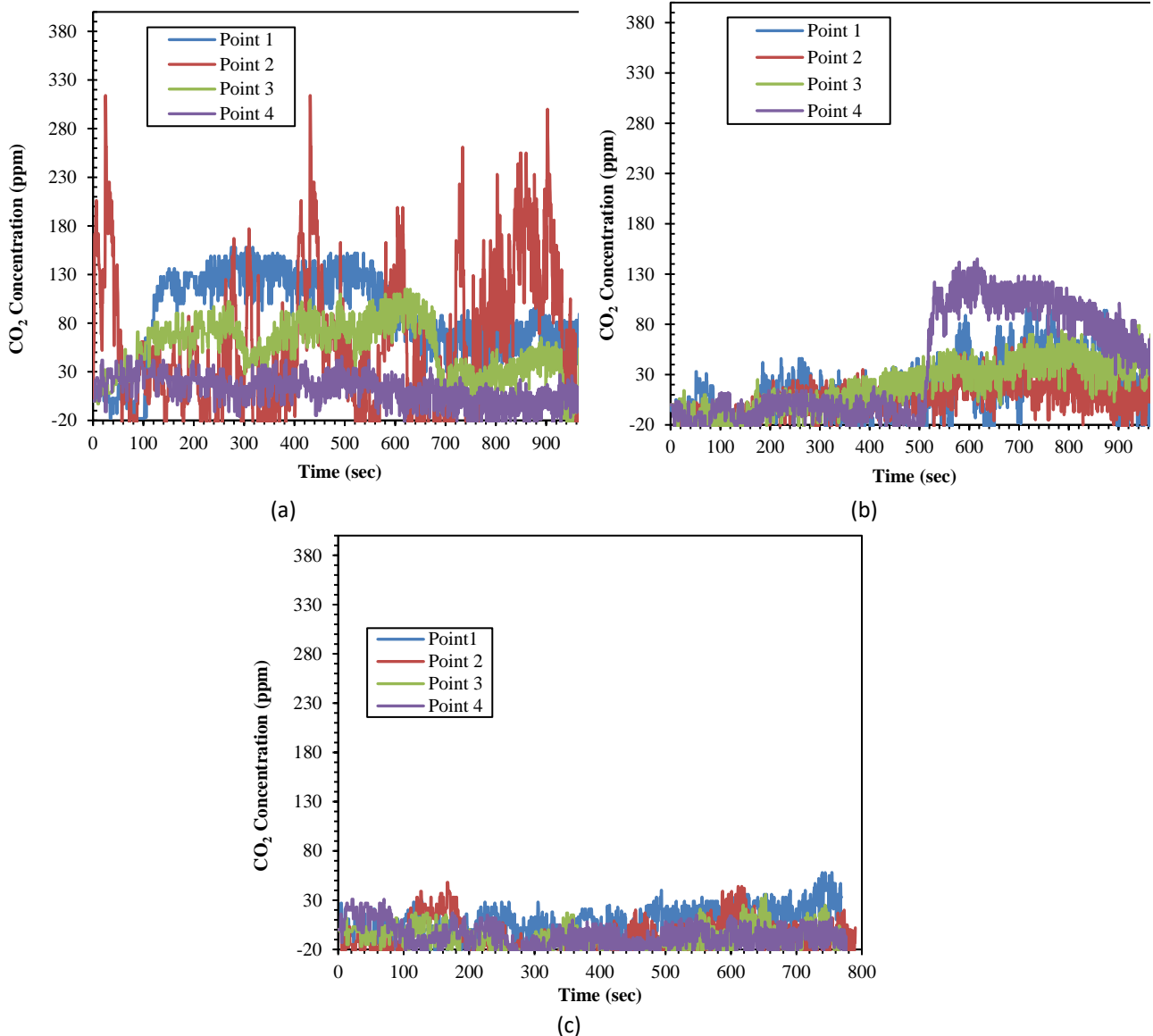
Fig. 5. CO_2 concentration with various strategies (a) Strategy 1, (b) Strategy 2, (c) Strategy 3

For strategy 2, the patient exhalation pressure increased with time, and some quantity of CO_2 got out through the ventilation outlet of the room. Contrary to strategy 1, the indoor air was mixed and spread slowly into the room due to the effects of thermal buoyancy, causing the airborne contaminants to be spread into the room. The average CO_2 concentrations at sample 2 (at the same level as the healthcare worker) for strategies 3, 2, and 1 were 4 ppm, 8 ppm, and 12 ppm, respectively. The uncertainty estimation of the sensor was evaluated and is explained in Table 4. The volume rendering concentration of CO_2 inside the potable chamber is shown in Figure 6. The concentration decreases with increasing the pressure difference. For strategy 1, CO_2 diffused inside the room due to buoyancy forces. Whereas, for the strategies with the portable chamber, the concentration did not diffuse due to the higher velocity that was created by the gaps, and the pressure difference between the inside of the portable chamber and the surrounding room air. The concentration decreases gradually with the pressure difference for the six strategies.
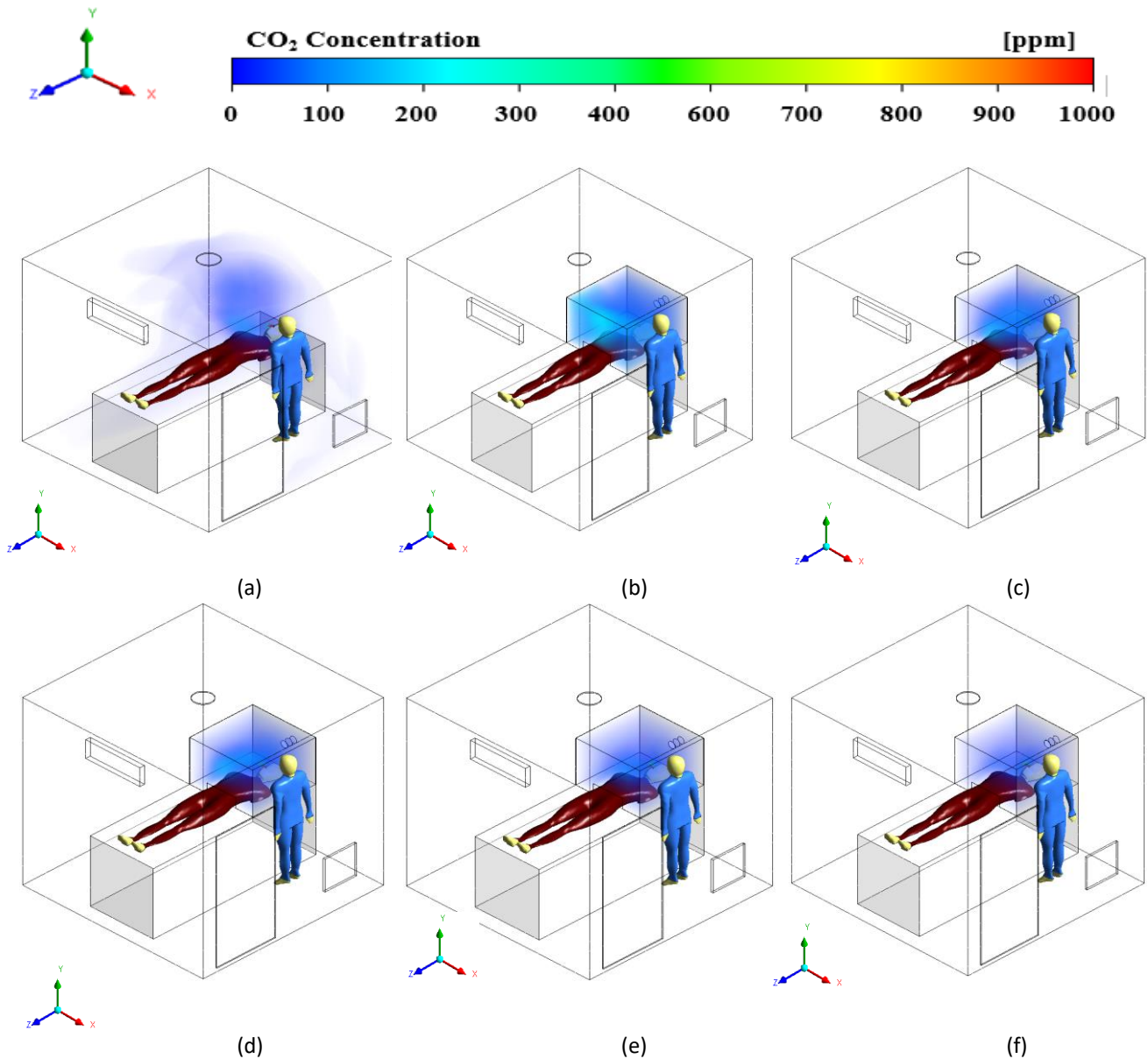
Fig. 6. Contours of CO_2 concentration with constant 27 ACH at 60.3 s, (a) Strategy 1, (b) Strategy 2, (c) Strategy 3, (d) Strategy 4, (e) Strategy 5, (f) Strategy 6

4.3 Comparisons with Related Previous Work

This study suggests a modification that can be implemented in any suitable room (in a hospital or even at home) at a low cost. The purpose of the modification is to reduce the area of infection containment to prevent its spread within the room by placing a portable chamber above the patient on the bed to control the infection and reduce its spread distance inside the patient room. Through the exhaust opening of the portable room behind the patient, airborne carbon dioxide was sucked from the chamber using a vacuum pump. Table 5 presents some studies related to the location of the room exhaust and its effect on the average concentration of the tracer gas inside the chamber.

Table 5
Effect of location of exhaust air opening on the concentration of air suspensions

Position of inlet and outlet	Dimensions (L×W× H)	Methodology	Mean Concentration (ppm)	Ref.
Ceiling supply air (SA) and exhaust air (EA) 0.2m above the floor.	4m x 4m × 2.6 m	Pollutant distribution was investigated using numerical simulations with three ventilation strategies analyzed based on exhaust air locations using gas trace SF6.	37.4	[29]
Ceiling SA and ceiling EA.			48.4	
Ceiling SA and the two wall-mounted EA behind the patient's head.			34.8	
Two air supply diffusers and two extract grilles are mounted on the ceiling.	3.35m × 4.8m × 2.6 m	Using gas trace SF6 to represent the emission source at a rate of 0.63 l/min. The average concentration was measured at sampling points (six).	64.4	[37]
Two SA diffusers are mounted on the ceiling and two EA grilles to the wall behind the bed at 0.3m above the floor level.			31.3	
Two SA diffusers are mounted on the wall behind the bed and two EA grilles to the wall behind the bed at 0.3m above the floor level.			29	
One SA opening at the bottom left and two EA openings, one at the top right and the other at the bottom right.	two-dimensional 2.0m × 1.0m	Evaluate the effects of velocity ratios between the exhaust ratio (0.1:0.9, 0.3:0.7, 0.5:0.5, and 0.7: 0.3).	Concentration is less than 45 ppm	[38]
SA was mounted on the wall and EA was mounted on the opposite wall.	3.8m × 4m × 2.4m	Studied the relative concentration between two persons face to face with the relative distance of 1m in three cases: Stable, unstable, and neutral	560 – 600 ppm for stable 480 -500 ppm for unstable 490 -520 ppm for neutral	[39]
Ceiling SA and EA were located lower wall behind the head patient.	3.7m × 2.5m × 2.5m	Studied the concentration of gas exhaled from the patient with different air changes per hour (12 - 48) in the case of an opening door of the isolation room.	48.811 to 50.81 ppm for 12 ACH 13.19 to 13.40 ppm for 48 ACH	[40]
SA was mounted in the wall near the ceiling and EA was mounted inside the wall to the left of the patient above the floor by 0.25m.	2m × 2m × 2m	Case study without portable chamber with 27 ACH. Case study with portable chamber and 27 ACH.	47 ppm 1 ppm	Present study

4.4 Velocity Contours

The velocity contours around the patient at the two heights of 0.9 m and 1 m are shown in Figure 7. The average velocity, for all strategies at the height of 1 m near the patient, was less than 0.25 m/s, which is the recommended value [27]. In addition, at the height of 0.9 m, the velocities for strategies 1 and 2 were less than the recommended value.

For other strategies, the velocity at this height increased around the patient with increasing the pressure difference at the exhaust of the portable chamber due to the increase of the air suction

from the gap. The purpose of the gap is to prevent infection from spreading from the portable chamber to the original room (surrounding healthcare workers). It serves as a small isolation room for the patient.
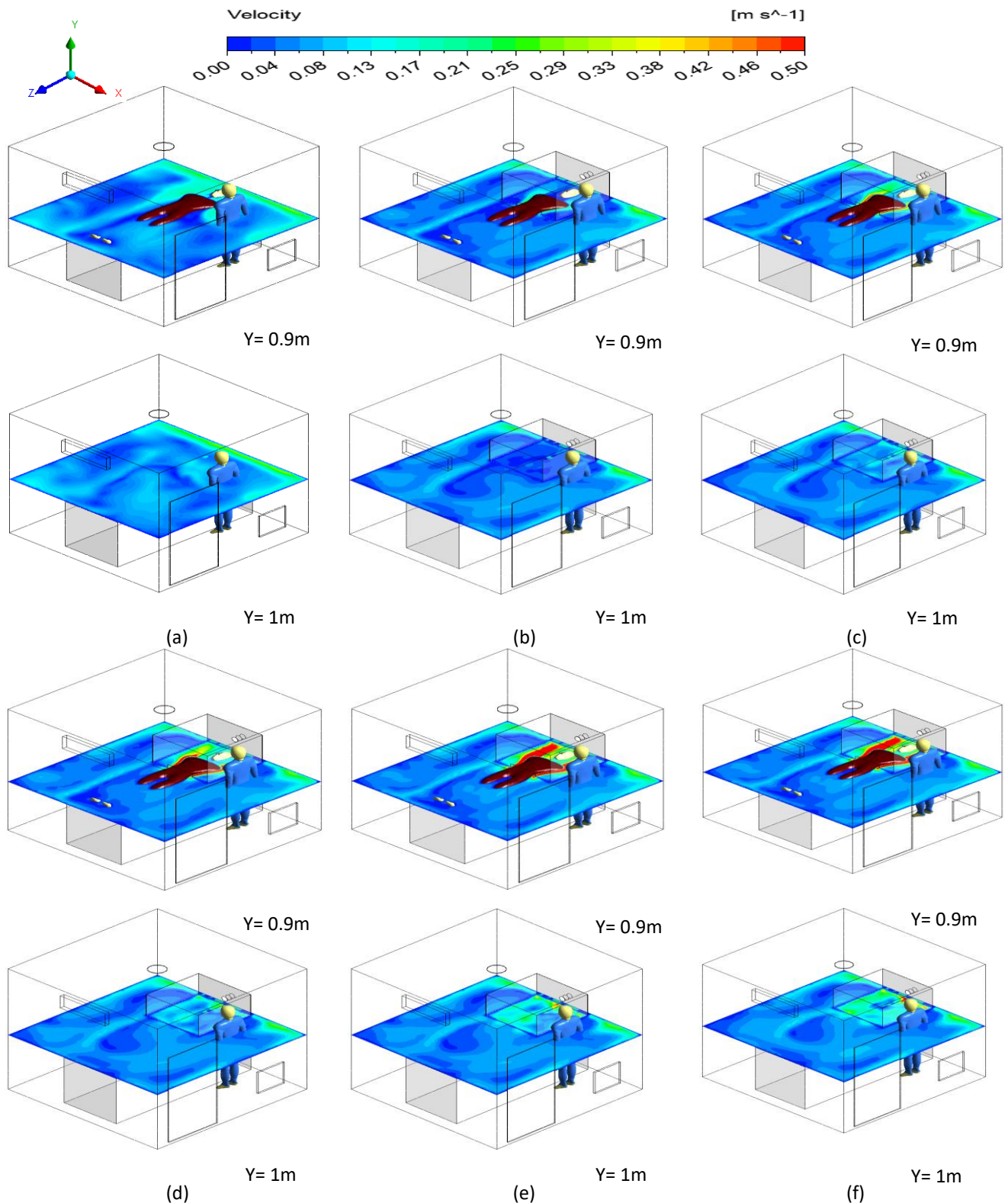
Fig. 7. Velocity contours with different pressure values at the exhaust 2 (a) Strategy 1, (b) Strategy 2, (c) Strategy 3, (d) Strategy 4, (e) Strategy 5, (f) Strategy 6

4.5 Water Droplet Diameter

The water droplet diameter for the six strategies is illustrated in Figure 8. For strategy 1, the droplets diffused inside the room and around the healthcare worker quickly. The droplet diameter inside the room was lower than 3×10^{-7} mm. For other strategies, the water droplets diffused inside the portable chamber and were controlled using the vacuum pump to prevent from spreading to the healthcare worker. The droplet diameter range inside the portable chamber was lower than 7×10^{-7} mm. The velocity at the gaps prevented the infection spread to the healthcare worker and pushed the infection towards the portable chamber exhaust. The infection exiting from the exhaust was passed through ultraviolet (UV) devices to kill the viruses.
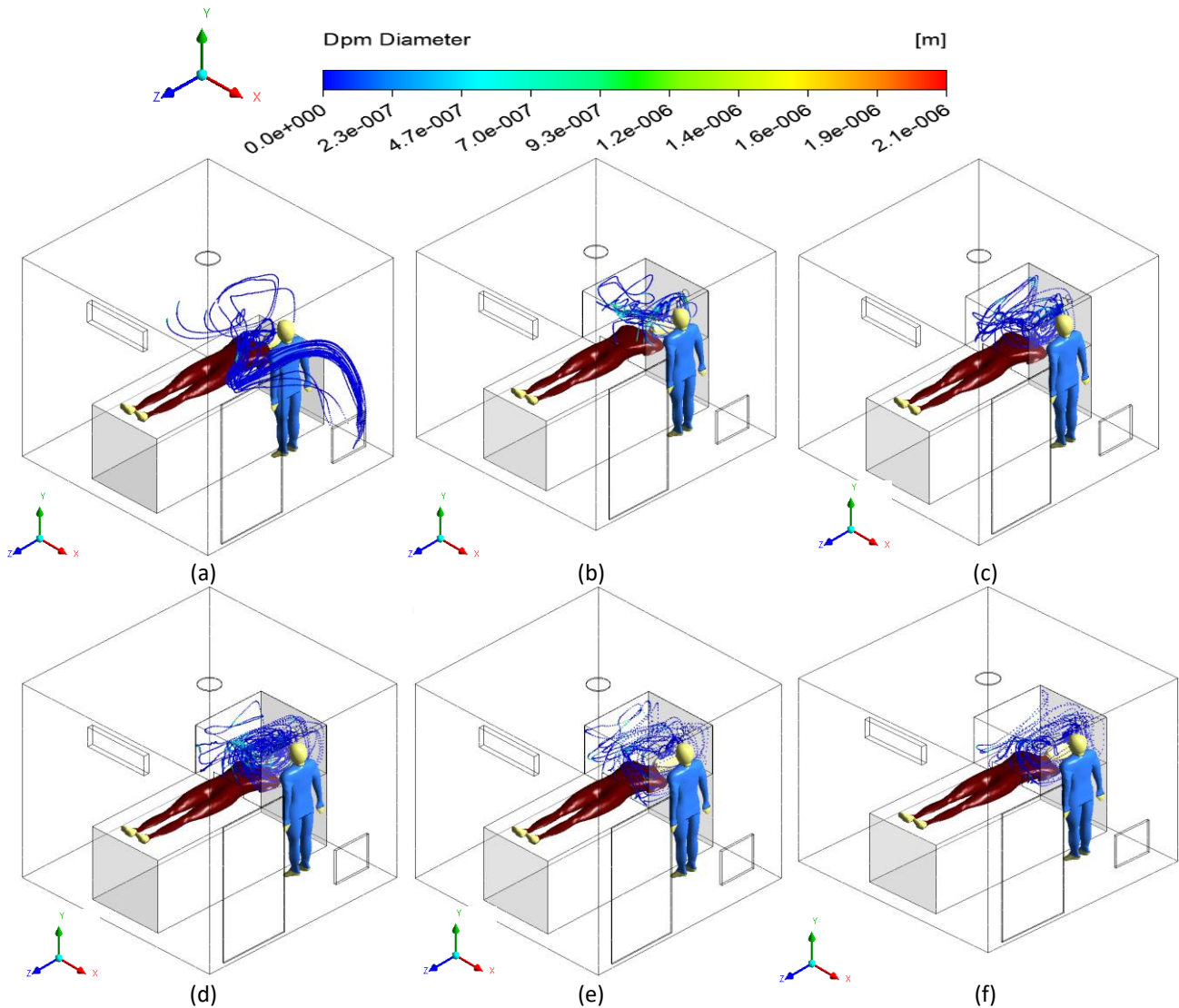
Fig. 8. Water aerosol diameter from patient exhalation with constant 27 ACH (a) Strategy 1, (b) Strategy 2, (c) Strategy 3, (d) Strategy 4, (e) Strategy 5, (f) Strategy 6

4.6 Droplet Residence Time

Figure 9 clearly shows that the portable chamber air exhaust behind the patient is efficient in removing fine particles, and the removal of large particles is highly dependent on the pressure difference, as explained earlier, and is apparent in strategy 6. Fine particles can remain suspended in the air for a long time and may be transported a long distance, whereas large particles cannot.

Additionally, with higher relative humidity, the fine droplets evaporation process is slower, and vice versa [41]. Moreover, the social distance is dependent on the size of particles, as shown in Table 6, with smaller particles requiring a longer social distance. While using a portable chamber, the particle sizes didn't mix with the indoor air.
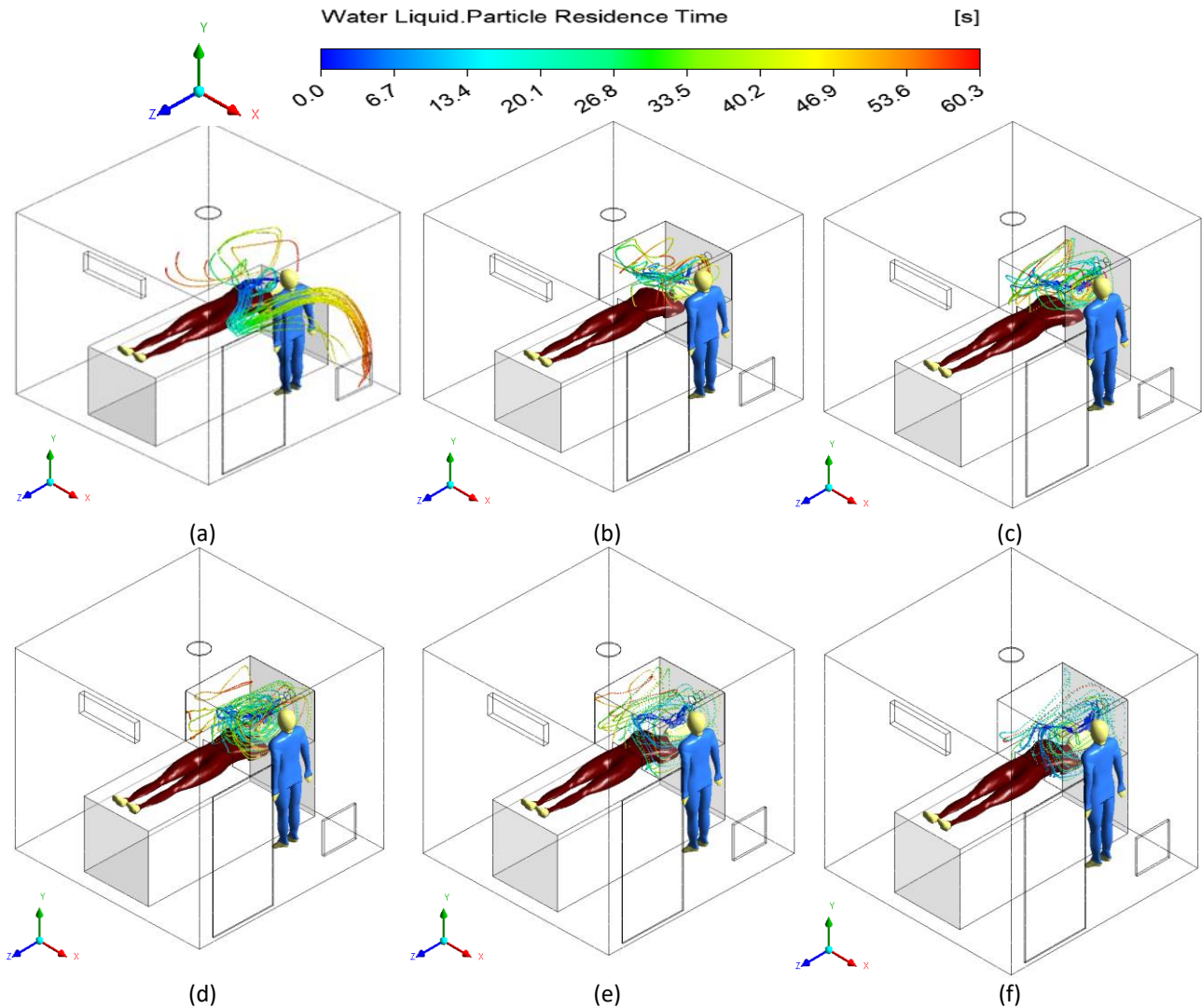
Fig. 9. Water aerosol time residence from patient exhaled with constant 27 ACH (a) Strategy 1, (b) Strategy 2, (c) Strategy 3, (d) Strategy 4, (e) Strategy 5, (f) Strategy 6

Table 6
The social distance according to droplet diameters

Type state	Droplet diameter (μm)	ACH/ Velocity	Social distance (m)	Time residence (sec)	Ref(s).
Exhaled breathing	10	-	≤ 1	300	[42-44]
	1	-	≥ 2	30,000	[42-44]
Exhaled breathing	1	27	0.3	60.3	Present study

5. Ventilation Effectiveness

The performance of the portable chamber at a significant point near the patient inside the original chamber is shown in Figure 10. Considering the average value of pollutant concentration at the significant point dimension (1.1 m, 1.2 m, and 0.7 m), as shown in Figure 3(b), strategy 1 had a higher concentration value, which ranged between 50 and 250 ppm. In contrast, strategy 6 was more effective than strategies 2, 3, 4, and 5 in removing pollutants from the room by percentages of 61.6%, 70.4%, 52.4%, and 33.0%, respectively. Although strategy 6 was better than other strategies, its use is not recommended. This is because the velocity is sometimes higher than the recommended value of 0.25 m/s [27] around the patient in addition to the high turbulence intensity, which was reflected in the method of disposal of small-diameter particle drops. With the turbulent intensity increasing, the fine particles can remain suspended in the air for a longer time compared to the coarse ones.
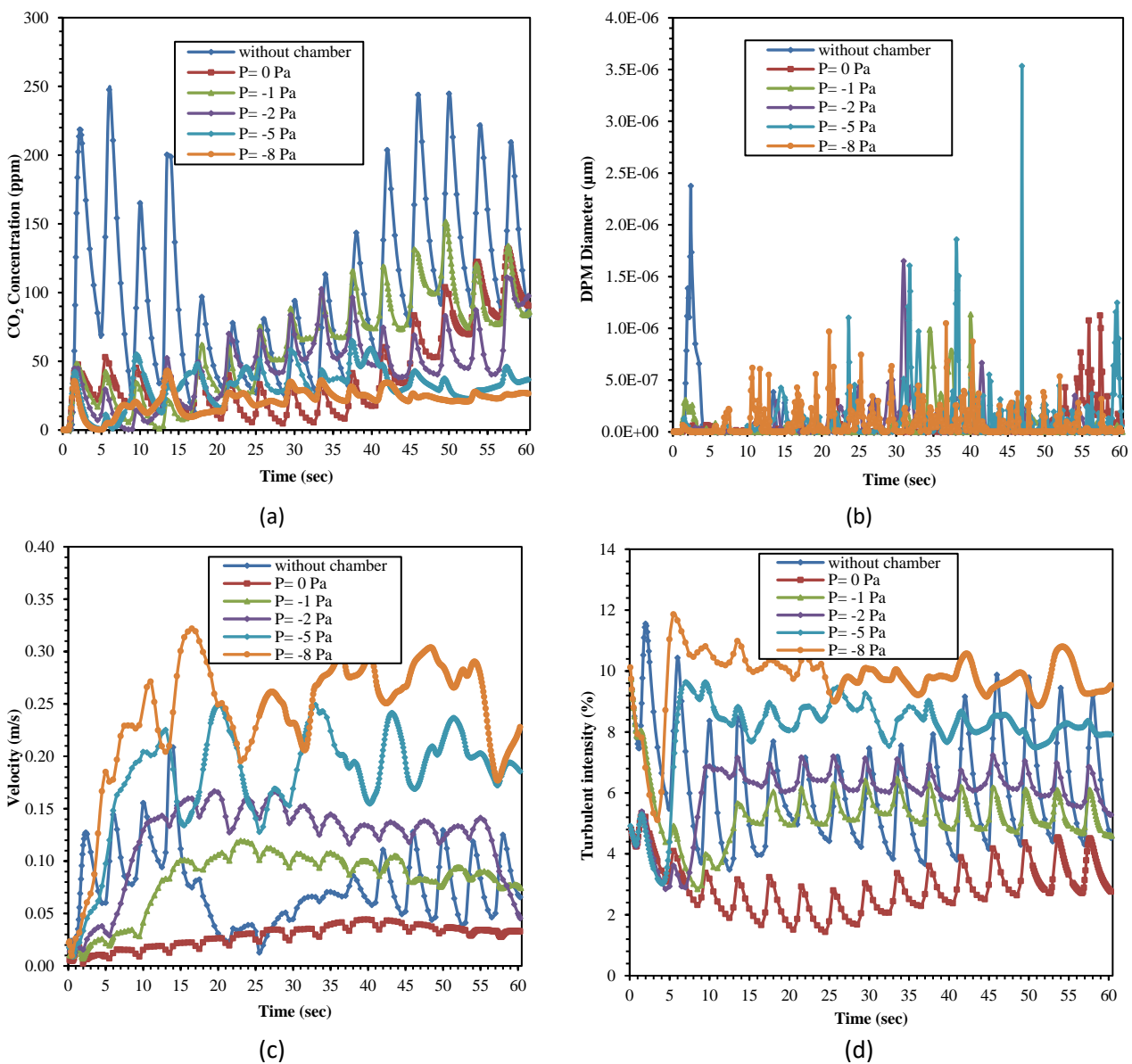
Fig. 10. Performance of portable chamber at the significant point with difference pressure at 60.3s (a) CO_2 concentration, (b) DPM diameter, (c) Velocity, (d) Turbulent intensity.

6. Conclusions

This study was conducted in a room containing one patient, a portable chamber above the patient, and a standing healthcare worker. The objective was to investigate the dispersion of the infection inside the portable chamber in addition to its effectiveness in minimizing the risk of infection for the healthcare worker. The portable chamber inside the room is a small isolation room, which is an efficient approach to reduce the spread of particles inside the room to the nearby healthcare worker. It is also easy to implement and can be used in different environments to avoid the spread of infection. From the previously presented and discussed results, the following conclusions may be put forward

    i.   The gaps (distance between the patient and portable chamber) velocity and creating negative pressurization across the chamber entrance are necessary for preventing particulate spread.

    ii.   The removal of large particles is highly dependent on the pressure difference. Fine particles can remain suspended in the air for a long time and can be transported a long distance. The time residence of the fin particle decreases with increasing the pressure difference inside the potable chamber.

    iii.   Although strategy 6 is better than other strategies, its use is not recommended because the velocity is higher than the recommended value of 0.25 m/s at Y = 0.9 m [27]. Therefore, it is preferable to use strategies 5 to 2 because the value of velocity around the patient does not exceed the recommended value.

    iv.   The results of this study indicate that the portable chamber is effective in reducing airborne infection because the CO_2 concentration and the velocity around the patient do not exceed the maximum limit by OSHA standards [27]. In addition, it prevents the diffusion of small particles in indoor air.

References

[1] Van Doremalen, Neeltje, Trenton Bushmaker, Dylan H. Morris, Myndi G. Holbrook, Amandine Gamble, Brandi N. Williamson, Azaibi Tamin et al. "Aerosol and surface stability of SARS-CoV-2 as compared with SARS-CoV-1." *New England journal of medicine* 382, no. 16 (2020): 1564-1567. https://doi.org/10.1056/NEJMc2004973

[2] Induri, Sri Nitya Reddy, Yunah Caroline Chun, Joonmo Christopher Chun, Kenneth E. Fleisher, Robert S. Glickman, Fangxi Xu, Efthimia Ioannidou, Xin Li, and Deepak Saxena. "Protective measures against COVID-19: Dental practice and infection control." In *Healthcare*, vol. 9, no. 6, p. 679. Multidisciplinary Digital Publishing Institute, 2021. https://doi.org/10.3390/healthcare9060679

[3] World Health Organization, (2020. *Transmission of SARS-CoV-2: implications for infection prevention precautions: scientific brief, 09 July 2020*. No. WHO/2019-nCoV/Sci_Brief/Transmission_modes/2020.3. World Health Organization, 2020.

[4] Kalliomäki, Petri, Kim Hagström, Harri Itkonen, Ismo Grönvall, and Hannu Koskela. "Effectiveness of directional airflow in reducing containment failures in hospital isolation rooms generated by door opening." *Building and Environment* 158 (2019): 83-93. https://doi.org/10.2514/6.2015-1229

[5] Mousavi, Ehsan S., and Kevin R. Grosskopf. "Ventilation rates and airflow pathways in patient rooms: A case study of bioaerosol containment and removal." *Annals of Occupational Hygiene* 59, no. 9 (2015): 1190-1199. https://doi.org/10.1093/annhyg/mev048

[6] Qian, Hua, and Xiaohong Zheng. "Ventilation control for airborne transmission of human exhaled bio-aerosols in buildings." *Journal of thoracic disease* 10, no. Suppl 19 (2018): S2295. https://doi.org/10.21037/jtd.2018.01.24

[7] Somsen, G. Aernout, Cees van Rijn, Stefan Kooij, Reinout A. Bem, and Daniel Bonn. "Small droplet aerosols in poorly ventilated spaces and SARS-CoV-2 transmission." *The Lancet Respiratory Medicine* 8, no. 7 (2020): 658-659. https://doi.org/10.1016/S2213-2600(20)30245-9

[8] Adir, Yochai, Ori Segol, Dmitry Kompaniets, Hadas Ziso, Yechiam Yaffe, Irina Bergman, Erez Hassidov, and Arieh Eden. "COVID-19: minimising risk to healthcare workers during aerosol-producing respiratory therapy using an

innovative constant flow canopy." *European Respiratory Journal* 55, no. 5 (2020). https://doi.org/10.1183/13993003.01017-2020

[9] Lin, Zhang, Jinliang Wang, Ting Yao, and Tin Tai Chow. "Investigation into anti-airborne infection performance of stratum ventilation." *Building and Environment* 54 (2012): 29-38. https://doi.org/10.1016/j.buildenv.2012.01.017

[10] Feng, Zhuangbo, and Shi-Jie Cao. "A newly developed electrostatic enhanced pleated air filters towards the improvement of energy and filtration efficiency." *Sustainable Cities and Society* 49 (2019): 101569. https://doi.org/10.1016/j.scs.2019.101569

[11] Feng, Zhuangbo, Junyan Yang, and Jie Zhang. "Numerical optimization on newly developed electrostatic enhanced pleated air filters for efficient removal of airborne ultra-fine particles: Towards sustainable urban and built environment." *Sustainable Cities and Society* 54 (2020): 102001. https://doi.org/10.1016/j.scs.2019.102001

[12] Ren, Jianlin, Michael Wade, Richard L. Corsi, and Atila Novoselac. "Particulate matter in mechanically ventilated high school classrooms." *Building and Environment* 184 (2020): 106986. https://doi.org/10.1016/j.buildenv.2020.106986

[13] Doughty, David C., Steven C. Hill, and Daniel W. Mackowski. "Viruses such as SARS-CoV-2 can be partially shielded from UV radiation when in particles generated by sneezing or coughing: Numerical simulations." *Journal of Quantitative Spectroscopy and Radiative Transfer* 262 (2021): 107489. https://doi.org/10.1016/j.jqsrt.2020.107489

[14] Feng, Zhuangbo, Shi-Jie Cao, and Fariborz Haghighat. "Removal of SARS-CoV-2 using UV+ Filter in built environment." *Sustainable Cities and Society* 74 (2021): 103226. https://doi.org/10.1016/j.scs.2021.103226

[15] Beggs, Clive B., and Eldad J. Avital. "Upper-room ultraviolet air disinfection might help to reduce COVID-19 transmission in buildings: a feasibility study." *PeerJ* 8 (2020): e10196. https://doi.org/10.7717/peerj.10196

[16] Luo, Na, Wenguo Weng, Xiaoyu Xu, and Ming Fu. "Human-walking-induced wake flow–PIV experiments and CFD simulations." *Indoor and Built Environment* 27, no. 8 (2018): 1069-1084. https://doi.org/10.1177/1420326X17701279

[17] Weiser, Mitchell C., Shai Shemesh, Darwin D. Chen, Michael J. Bronson, and Calin S. Moucha. "The effect of door opening on positive pressure and airflow in operating rooms." *JAAOS-Journal of the American Academy of Orthopaedic Surgeons* 26, no. 5 (2018): e105-e113. https://doi.org/10.5435/JAAOS-D-16-00891

[18] Kalliomäki, Petri, Pekka Saarinen, Julian W. Tang, and Hannu Koskela. "Airflow patterns through single hinged and sliding doors in hospital isolation rooms–Effect of ventilation, flow differential and passage." *Building and Environment* 107 (2016): 154-168. https://doi.org/10.1016/j.buildenv.2016.07.009

[19] Haselton, F. R., and P. G. Sperandio. "Convective exchange between the nose and the atmosphere." *Journal of Applied Physiology* 64, no. 6 (1988): 2575-2581. https://doi.org/10.1152/jappl.1988.64.6.2575

[20] Chen, C., and Bin Zhao. "Some questions on dispersion of human exhaled droplets in ventilation room: answers from numerical investigation." *Indoor Air* 20, no. 2 (2010): 95-111. https://doi.org/10.1111/j.1600-0668.2009.00626.x

[21] Morawska, L. J. G. R., G. R. Johnson, Z. D. Ristovski, Megan Hargreaves, Kerrie Mengersen, Shay Corbett, Christopher Yu Hang Chao, Yuguo Li, and David Katoshevski. "Size distribution and sites of origin of droplets expelled from the human respiratory tract during expiratory activities." *Journal of aerosol science* 40, no. 3 (2009): 256-269. https://doi.org/10.1016/j.jaerosci.2008.11.002

[22] Chillón, Sergio A., Ainara Ugarte-Anero, Iñigo Aramendia, Unai Fernandez-Gamiz, and Ekaitz Zulueta. "Numerical modeling of the spread of cough saliva droplets in a calm confined space." *Mathematics* 9, no. 5 (2021): 574. https://doi.org/10.3390/math9050574

[23] Ren, Juan, Yue Wang, Qibo Liu, and Yu Liu. "Numerical study of three ventilation strategies in a prefabricated COVID-19 inpatient ward." *Building and Environment* 188 (2021): 107467. https://doi.org/10.1016/j.buildenv.2020.107467

[24] El-Haroun, Ahmed Fahmy, Sayed Ahmed Kaseb, Mahmoud Ahmed Fouad, and Hatem Omar Kayed. "Numerical Investigation of Covid-19 Infection Spread Expelled from Cough in an Isolation Ward Under Different Air Distribution Strategies." *Journal of Advanced Research in Fluid Mechanics and Thermal Sciences* 95, no. 1 (2022): 17-35. https://doi.org/10.37934/arfmts.95.1.1735

[25] Hatif, Ihab Hasan, Azian Hariri, and Ahmad Fu'ad Idris. "CFD analysis on effect of air Inlet and outlet location on air distribution and thermal comfort in small office." *CFD Letters* 12, no. 3 (2020): 66-77. https://doi.org/10.37934/cfdl.12.3.6677

[26] Winata, I. Made Putra Arya, Putu Emilia Dewi, Putu Brahmanda Sudarsana, and Made Sucipta. "Air-Flow Simulation in Child Respirator for Covid-19 Personal Protection Equipment Using Bamboo-Based Activated Carbon Filter." *Journal of Advanced Research in Fluid Mechanics and Thermal Sciences* 91, no. 1 (2022): 83-91. https://doi.org/10.37934/arfmts.91.1.8391

[27] Tungjai, A., and K. Kubaha. "Indoor air quality evaluation of isolation room for hospital in Thailand." *Energy procedia* 138 (2017): 858-863. https://doi.org/10.1016/j.egypro.2017.10.100

[28] Ismail, A. M. M., N. A. S. Manssor, N. Amilin, A. Nalisa, I. Izyan, and N. Yahaya. "Dust Concentration in Office Environment." *Journal of Advanced Research in Applied Mechanics* 13 (2020): 1-11. https://www.akademiabaru.com/doc/ARAMV13_N1_P1_11.pdf

[29] Cho, Jinkyun. "Investigation on the contaminant distribution with improved ventilation system in hospital isolation rooms: Effect of supply and exhaust air diffuser configurations." *Applied thermal engineering* 148 (2019): 208-218. https://doi.org/10.1016/j.applthermaleng.2018.11.023

[30] Chen, C., and Bin Zhao. "Some questions on dispersion of human exhaled droplets in ventilation room: answers from numerical investigation." *Indoor Air* 20, no. 2 (2010): 95-111. https://doi.org/10.1111/j.1600-0668.2009.00626.x

[31] Morawska, L. J. G. R., G. R. Johnson, Z. D. Ristovski, Megan Hargreaves, Kerrie Mengersen, Shay Corbett, Christopher Yu Hang Chao, Yuguo Li, and David Katoshevski. "Size distribution and sites of origin of droplets expelled from the human respiratory tract during expiratory activities." *Journal of aerosol science* 40, no. 3 (2009): 256-269. https://doi.org/10.1016/j.jaerosci.2008.11.002

[32] Wang, B., A. Zhang, J. L. Sun, H. Liu, J. Hu, and L. X. Xu. "Study of SARS transmission via liquid droplets in air." *Journal of biomechanical engineering* 127, no. 1 (2005): 32-38. https://doi.org/10.1115/1.1835350

[33] Liu, Yuan, Zhi Ning, Yu Chen, Ming Guo, Yingle Liu, Nirmal Kumar Gali, Li Sun et al. "Aerodynamic analysis of SARS-CoV-2 in two Wuhan hospitals." *Nature* 582, no. 7813 (2020): 557-560. https://doi.org/10.1038/s41586-020-2271-3

[34] Villafruela, J. M., Inés Olmedo, M. Ruiz De Adana, C. Méndez, and Peter V. Nielsen. "CFD analysis of the human exhalation flow using different boundary conditions and ventilation strategies." *Building and Environment* 62 (2013): 191-200. https://doi.org/10.1016/j.buildenv.2013.01.022

[35] Villafruela, J. M., I. S. J. J. Olmedo, and J. F. San José. "Influence of human breathing modes on airborne cross infection risk." *Building and Environment* 106 (2016): 340-351. https://doi.org/10.1016/j.buildenv.2016.07.005

[36] Fohimi, Nor Azirah Mohd, Koay Mei Hyie, Salina Budin, Normariah Che Maideen, Nazri Kamsah, and Haslinda Mohamed Kamar. "An Experimental Study of Indoor Air Pollution in New Office Building." *Journal of Advanced Research in Fluid Mechanics and Thermal Sciences* 94, no. 1 (2022): 120-128. https://doi.org/10.37934/arfmts.94.1.120128

[37] Cheong, K. W. D., and S. Y. Phua. "Development of ventilation design strategy for effective removal of pollutant in the isolation room of a hospital." *Building and Environment* 41, no. 9 (2006): 1161-1170. https://doi.org/10.1016/j.buildenv.2005.05.007

[38] Hayashi, Tatsuya, Yoshiaki Ishizu, Shinsuke Kato, and Shuzo Murakami. "CFD analysis on characteristics of contaminated indoor air ventilation and its application in the evaluation of the effects of contaminant inhalation by a human occupant." *Building and Environment* 37, no. 3 (2002): 219-230. https://doi.org/10.1016/S0360-1323(01)00029-4

[39] Deng, Xiaorui, Guangcai Gong, Xizhi He, Xing Shi, and Lan Mo. "Control of exhaled SARS-CoV-2-laden aerosols in the interpersonal breathing microenvironment in a ventilated room with limited space air stability." *journal of environmental sciences* 108 (2021): 175-187. https://doi.org/10.1016/j.jes.2021.01.025

[40] Tung, Yun-Chun, Yang-Cheng Shih, and Shih-Cheng Hu. "Numerical study on the dispersion of airborne contaminants from an isolation room in the case of door opening." *Applied Thermal Engineering* 29, no. 8-9 (2009): 1544-1551. https://doi.org/10.1016/j.applthermaleng.2008.07.009

[41] Aliabadi, Amir A., Steven N. Rogak, Sheldon I. Green, and Karen H. Bartlett. "CFD simulation of human coughs and sneezes: a study in droplet dispersion, heat, and mass transfer." In *ASME International Mechanical Engineering Congress and Exposition*, vol. 44441, pp. 1051-1060. 2010. https://doi.org/10.1115/IMECE2010-37331

[42] Borro, Luca, Lorenzo Mazzei, Massimiliano Raponi, Prisco Piscitelli, Alessandro Miani, and Aurelio Secinaro. "The role of air conditioning in the diffusion of Sars-CoV-2 in indoor environments: a first computational fluid dynamic model, based on investigations performed at the Vatican State Children's hospital." *Environmental research* 193 (2021): 110343. https://doi.org/10.1016/j.envres.2020.110343

[43] Zayas, Gustavo, Ming C. Chiang, Eric Wong, Fred MacDonald, Carlos F. Lange, Ambikaipakan Senthilselvan, and Malcolm King. "Cough aerosol in healthy participants: fundamental knowledge to optimize droplet-spread infectious respiratory disease management." *BMC pulmonary medicine* 12, no. 1 (2012): 1-12. https://doi.org/10.1186/1471-2466-12-11

[44] Thatiparti, Deepthi Sharan, Urmila Ghia, and Kenneth R. Mead. "Computational fluid dynamics study on the influence of an alternate ventilation configuration on the possible flow path of infectious cough aerosols in a mock airborne infection isolation room." *Science and technology for the built environment* 23, no. 2 (2017): 355-366. https://doi.org/10.1080/23744731.2016.1222212